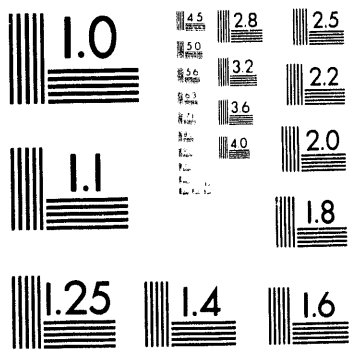
1.0
1.1
1.25
1.4
1.6
1.8
2.0
2.2
2.5
2.8
3.2
3.6
4.0
4.5
5.0
5.6
6.3
7.1

1 of 1

LBL-34700
UC-400

Characterization of Acoustic Effects on Flame Structures by Beam Deflection Technique.

Benoît Bédat, Larry W. Kostiuk, Robert K. Cheng

Energy and Environment Division
Lawrence Berkeley Laboratory
University of California
Berkeley, California 94720

October 1993

This work was supported by NASA Microgravity Sciences and Applications Division and NASA Lewis Research Center under contract No. C-32000-R through the U.S. Department of Energy Contract No. DE-AC03-76F00098.

Characterization of Acoustic Effects on Flame Structures by Beam Deflection Technique.

Benoît Bédat, Larry W. Kostiuk, Robert K. Cheng

Energy and Environment Division
Lawrence Berkeley Laboratory
University of California
Berkeley, California

Introduction

In a recent microgravity schlieren study of the influence of the gravity on the structure of premixed laminar and turbulent flames, Kostiuk et al [1] observed small amplitude flame wrinkling and movements near the tip of laminar Bunsen flames. These flame movements are found to be independent of the flow rate and equivalence ratio. Under normal gravity conditions, the flame motion is dominated by the well known pulsating flame phenomenon due to the motion of the unstable product/air interface which surrounds the flame cone. As a result, the small flame wrinkles and movements are less noticeable. In microgravity the large scale flame pulsation disappears and the small flame wrinkles become the only observable feature of the laminar flame. At first, these wrinkles were thought to be associated with flame front instabilities, Durox et al [2]. However, the flame wrinkles scales seen on the schlieren images are not those predicted from the Landau or thermal diffusive instabilities.

Flame/acoustic coupling may provide a more plausible explanation. The effects of acoustics on flame characteristics is well known in enclosed systems and in high power combustion chambers the coupling between the acoustic modes and the heat release [3] can cause sufficient noise and vibration to be destructive. For open flames, this coupling is not wellunderstood and often neglected. Hence experimental evidence of acoustic effects can easily be mis-interpreted or attributed to other causes. As demonstrated in a recently investigation of the acoustics characteristics of turbulent propane/air premixed Bunsen flame by Bédat et al [4], a strong coupling exists between the flame and the acoustic modes of the burner. The objective of this work is to show that the internal acoustics of the burner are responsible for the small wrinkles described above. The

natural frequency of the resonator (burner) is computed and experimentally verified. To measure the flame wrinkle frequencies for comparison with the resonance burner frequency, a laser beam deflection technique is developed. This simple technique is ideal for future microgravity experiments because it meets many of the microgravity experimental constraints such as a requirement for low laser power , simple optics and ease of alignment. The flame wrinkles generated by the acoustics influence premixed flame behavior by modifying the structure of the flame and need to be mitigated. It was found that the amplitude of the resonator frequency can be damped by partially filling the settling chamber with fiber glass, to absorb the acoustic waves.

Diagnostics and apparatus

The conical Bunsen type burner used for the experiments is constructed of a settling chamber and a converging nozzle (Figure 1). The exit diameter of the nozzle is 25 mm and the settling chamber diameter is 75 mm. The lengths of the settling chamber and of the converging nozzle are 200 and 80 mm respectively. The bottom part of the settling chamber below the screen (100 mm) is filled with glass beads to destroy the large turbulence structures in the incoming flow and avoid flash back. The design of the convergent nozzle is based on that developed by Morel [5] and it produces laminar flows with a uniform velocity distribution across the exit. A ring is fitted at the exit of the burner to stabilizelean premixed CH4/air flames.

The images shown in Figure 3 are obtained by schlieren visualization [6]. Schlieren's most appealing aspect for microgravity work is that it requires a relatively low power light source. The optics are also relatively simple and easy to align. The low acquisition rate of the CCD camera (30 Hz) does not allow frequency analysis to be performed over a wide range. To improve temporal resolution, a simple beam deflection technique was developed based the on schlieren principle but only with a single beam traversing the flame (figure 2). The laser is focused onto a schlieren stop and a photo-multiplier is placed behind the stop to analyze the modulation of the laser beam deflected by the temperature gradients. The light received by the photomultiplier is correlated to the movement of the flame front. The photo-multiplier signal output is connected to a computer which performs frequency analysis by FFT.

Results

Qualitative results

The three sets of schlieren images shown in the figure 3 are obtained in normal (top), inverse (middle) and microgravity (bottom) conditions. The four consecutive pictures correspond to the time evolution in 1/15 sec. (the images have been processed to render an effective framing rate of 60 HZ [6]). The equivalence ratio and the flow rate are 0.9 and .42 litre/s respectively. The schlieren images of the normal gravity flame (top row) are characterized by the flame cone shown at the center and the mushroom-shaped product/air interface which surrounds it. The product/air interface is unstable and 'pumps' the flame. The movement of the flame front cone is controlled by the motion of this interface. Flame flickering is due to the rise and fall of the flame tip. In inverse gravity conditions, the interface between the product and surrounding air is more stable than in the previous case but it also controls the dynamics of the flame cone. Under microgravity conditions (bottom row), due to the absence of gravity, the interface product/air is no longer visible, (note that a shadow of the schlieren lens is visible near the bottom due to a slight unavoidable misalignment of the optics during the free-fall experiments). Without free convection, the dynamics of the interface is controlled solely by the diffusion of heat therefore the interface does not have a sharp temperature gradient to be shown by schlieren.

Under normal gravity conditions (top), some flame wrinkling near the flame tip is clearly visible in frames two and four, whereas in frame one and three, this is not as apparent. This wrinkling appears intermittently. For the inverse gravity case (middle) these wrinkles are more persistent and their amplitudes seem to be larger than the normal gravity condition. In the microgravity condition (bottom), the flame front shows regular and symmetric wrinkles that are larger than in the two other cases. The existence of these wrinkles in all the cases and that the near unity Lewis number for the CH4/air mixture demonstrate that the hydrodynamic flame front instability and thermal diffusive instability are not responsible. The wrinkles are also found to be independent of the equivalence ratio and flow rate. The acoustics of the burner seem to be the only remaining significant phenomenon which could cause these flame wrinkles.

Acoustic characterization of the burner

Given the geometry of the burner and the contraction ratio of nine, it can be assumed to behave as an Helmholtz resonator. Generally, the equations used to estimate the resonance frequency do not take into account the converging nozzle form. The correction for the converging nozzle is given by the equation (1).

$$f = \frac{c}{2\pi} \times \sqrt{\frac{\pi r^{*2}}{V(1 + Kr^*)}} \quad [Hz] \qquad (1)$$

with $$K = 2.222 \times (\frac{r^*}{l} - 0.05) + 0.8$$

and $$\text{if } K > 1.8 \Rightarrow K = 1.8$$

$$\text{if } K < 1.8 \Rightarrow K = 0.8$$

Here r*, l, V and c are respectively the radius and the length of the converging nozzle, the volume of the settling chamber, and the speed of the sound (340 m/s in normal conditions). The correction factor K depends on the converging nozzle dimensions, and for this burner, K is equal to 1.041. The presence of the glass balls inside the settling chamber decreases the effective volume. When the bottom 100 mm of the settling chamber is filled with glass beads, the resonance frequency is equal to 187 Hz. If the converging nozzle dimensions are not taken in account, the equations found in the literature overestimate the value of the frequency (for example, the formula given in the reference [7] p289 gives 715 Hz).

An experimental verification is made with hot wire in the isothermal conditions with the same flow rate of .42 litre/sec i.e. the same as that of the flame. Though is better to use a microphone, this could not be done due to a lack of appropriate equipment. However the acoustic wave consists of a pressure and a velocity wave and so the acoustic velocity spectra has the same shape as the acoustic pressure spectra. Figure 4 shows the velocity spectra obtained at the exit of the burner on the centerline for two cases : (1) part of the settling chamber is filled with glass beads and (2) with fiber glass to damp the acoustic waves. The velocity spectrum with the glass beads has several peaks. The most energetic is at a frequency of 180 Hz. This peak corresponds well to

the estimation of the Helmholtz resonator frequency. It is found that the resonator frequency does not change with increasing exit velocity and is not related to aerodynamic instabilities (i.e. a von Karman street behind the flame ring holder or jet instabilities). The others peaks at higher frequencies represent noise associated with the injection of the mixture at the bottom at the burner and with aerodynamic sound generated around the glass beads. Substituting the glass beads with the fiber glass decreases the level of the Helmholtz resonator frequency by a factor of 2 and the noise level at higher frequencies by a two orders of magnitudes. The inset in the top left of figure 4 shows the damping of the Helmholtz resonator frequency by the fiber glass. The peak at lower frequencies (60 Hz) is due to the electronic noise.

Beam deflection results

The beam deflection signal is proportional to the temperature gradients perpendicular to the laser beam path. The schlieren stop blocks all the non deflected laser beam and the photo multiplier receives only the deflected light. Even if the schlieren stop is not well-centered with the respect to the laser beam, the system response is not affected significantly because each flame front tends to generate the same deflection and the schlieren stop is small compared to the magnitude of this deflection. The system has a spatial resolution determined by the laser beam diameter (2mm). This seems large compared to the fluctuation amplitudes of the flame front. Image analysis of the schlieren pictures (figure 3) gives a rms value of the flame front position fluctuations of 0.3 mm for many locations [6]. Each flame movement induces a large beam deflection which is easily detected by the photo multiplier and so the normalized spectrum is a good representative of the temporal behavior of the flame. Note that the rms. value of the photomultiplier signal has no physical significance.

Figure 5 (a) compares the beam deflection spectra obtained with the glass beads and the fiber glass at half of flame cone height in the flame front zone (x/D = 0.63, r/D = 0.18) for the same equivalence ratio and flow rate given above, under normal gravitational conditions. The spectra consist of two peaks. The first has a frequency of 16 Hz and is related to the product/air interface in agreement with the qualitative results obtained from the schlieren images. Some harmonics of the 16 Hz also appear. The second peak is centered around 187 Hz (glass beads) and 165 Hz (fiber glass). Because the spectra are normalized by the rms values, it is difficult to use the comparison to determine if the apparent damping and shifting are due to the physics or to the diagnostic. In Figure 5 (b), the acoustic velocity spectra are plotted in normalized form. This figure shows the

same damping and shifting as in Figure 5 (a). Comparison between the beam deflection and acoustic measurements demonstrates clearly that the internal acoustics of the burner is the cause of the small scale wrinkles on the flame front. To demonstrate that the peak at 16 Hz shown in the figure 5 (a) is related only to product/air interface, Figure 6 shows the beam deflection spectrum in the product/air interface zone at the same height. This spectrum has only one peak at 16 Hz with its harmonics. The fact that a 16 Hz peak is found in the product/air interface and in the flame front zone demonstrates strongly a coupling in accord with the conclusion of the schlieren analysis [6].

Figure 7 shows the full beam deflection spectrum of Figure 5 (a). Except for the two peaks described above, there are no other significant fluctuation frequencies of the flame front. The only motion of the flame in this burner is due to the acoustic effect and the buoyancy driven instabilities. A perforated plate at the exit of the burner generates a turbulent flow. The flame is then also wrinkled by the turbulence. The perforated plate used in the experiments has hole diameters of 2mm and gives a turbulent intensity around 7 % and a length scale of ~3 mm. This set-up produces wrinkled laminar flames. Figure 8 shows a beam deflection spectrum obtained in the turbulent brush of this flame. The equivalence ratio is 0.7 and the flow rate is the same as for the laminar flame shown previously. The two peaks (16 and 180 Hz) are again visible and the background level corresponding to the flame wrinkles is higher than in the laminar case (Figure 7). This spectrum has the same shape as the velocity spectra obtained by L.D.V. in combusting conditions [1]. The beam deflection technique is able to measure the time scale of the turbulent flame wrinkles.

Conclusion

This work shows that the acoustic effects are the causes of the small amplitude flame wrinkling and movements seen in all the different gravitational conditions. The comparison between the acoustic velocity and beam deflection spectra for the two conditions studied (glass beads and fiber glass) demonstrates clearly this flame/acoustic coupling.

This acoustic study shows that the burner behaves like a Helmholtz resonator. The estimated resonance frequency corresponds well to the experimental measurements. The fiber glass damps the level of the resonance frequency and the flame motion. The changes shown in normalized beam deflection spectra give further support of this damping. This work demonstrates that the acoustics has a direct influence on flame

structure in the laminar case and the preliminary results in turbulent case also show a strong coupling.

The nature of this flame/acoustic coupling are still not well understood. Further investigation should include determining the frequency limits and the sensitivity of the flame to acoustic perturbations.

Acknowledgments

This work is supported by NASA Microgravity Sciences and Applications Division. Technical support is provided by NASA Lewis Research Center under contract No. C-32000-R through the U.S. Department of Energy Contract No. DE-AC03-76F00098.This visit of the first author to LBL is sponsored by French Research Ministry.

References

1. Kostiuk, L.W.; Zhou, L.; Cheng, R. 1992 : The effect of Gravity on Wrinkled Laminar flames, Western States Section. The Combustion Institute.

2. Durox, D., Baillot, B., Scoufflaire, P. and Prud'homme, R. 1990: Some Effects of Gravity on the Behavior of Premixed Flames, Combustion and Flame, Vol. 82, p.66.

3. Poinsot, T 1987 : Analyse des instabilités de combustion des foyers turbulents prémélangés, Thèse d'Etat, Université Paris Sud.

4. Bédat, B.; Giovannini, A.; Pauzin, S . 1993a :Thin Filament Infrared Pyrometry : Instantaneous Temperature Profile Measurements in a Weakly Turbulent Hydrocarbon Premixed Flame, Accepted in Experiments in Fluids.

5. Morel, T. 1975 : Comprehensive design of Axisymmetric wind tunnel contractions, Journal of Fluids Engineering. Trans. ASME Series I, Vol. 97, 225-233.

6. Kostiuk, L.W.; Cheng, R. 1993 : Imaging of Premixed Flames in Microgravity, submitted to Experiments in Fluids.

7. Morse, P. M.; Ingard, K. U. 1698 : Theoretical Acoustics, Mac Graw-Hill.

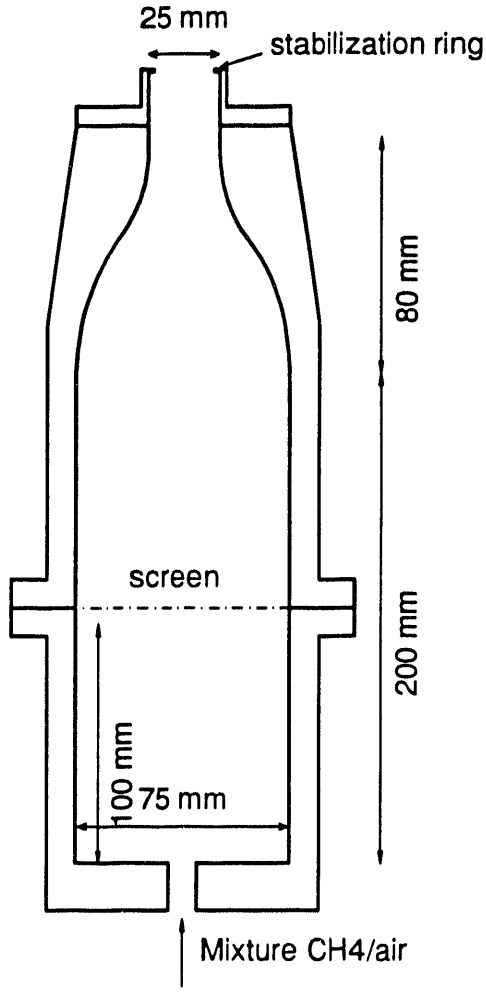

Figure 1 : Burner scheme

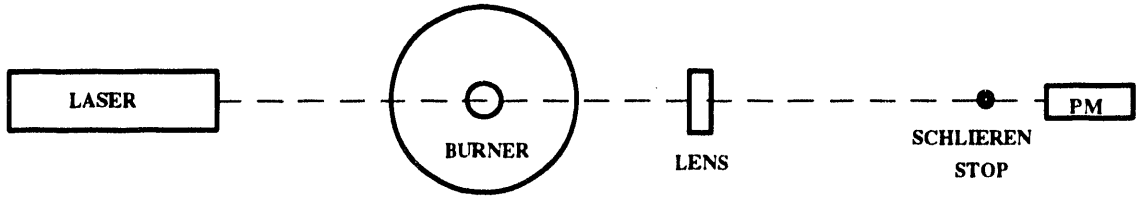

Figure 2 : Beam deflection technique set up

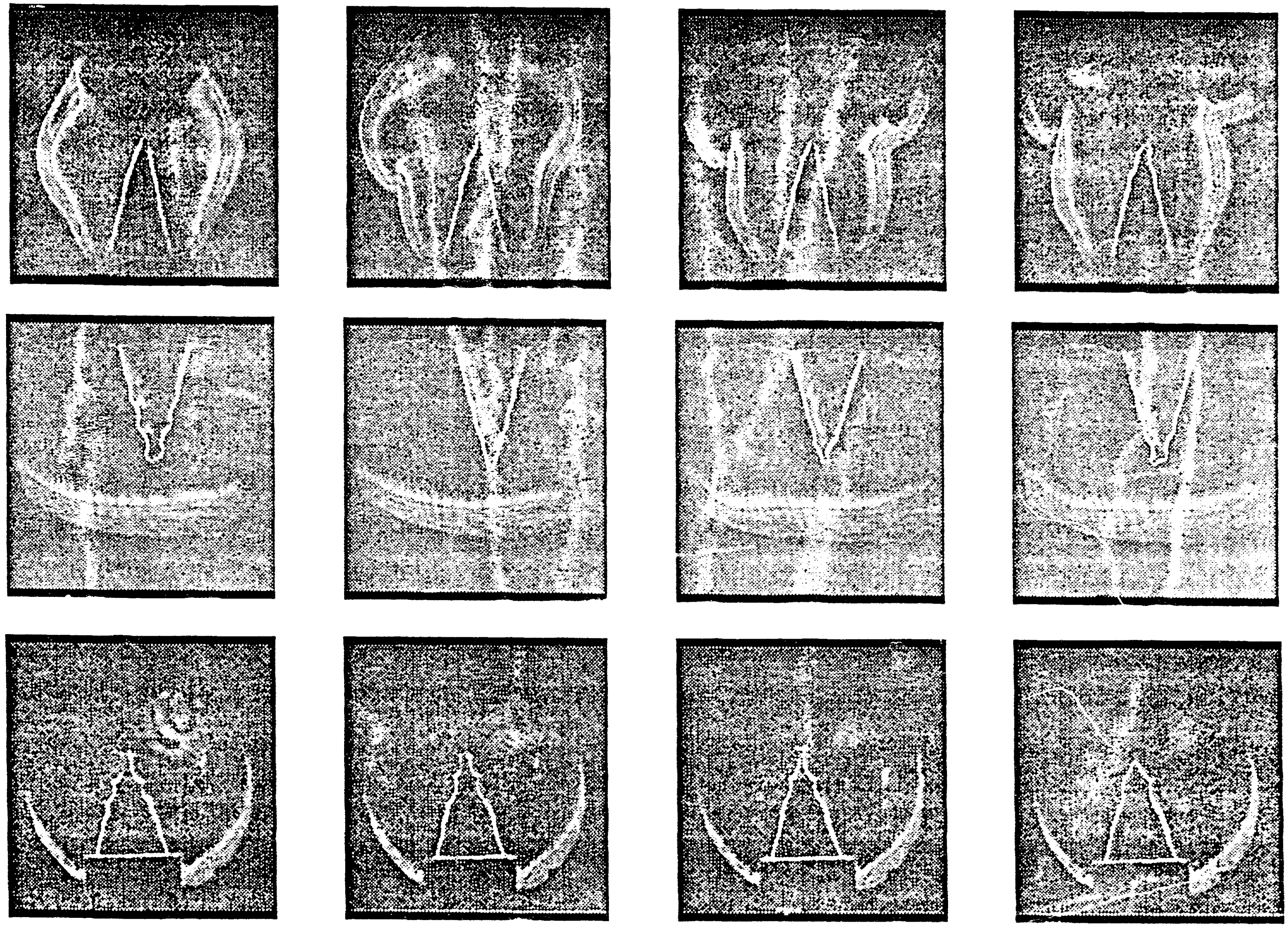

Figure 3 - Schlieren images in normal gravity (top), inverse gravity (middle) and microgravity (bottom) conditions

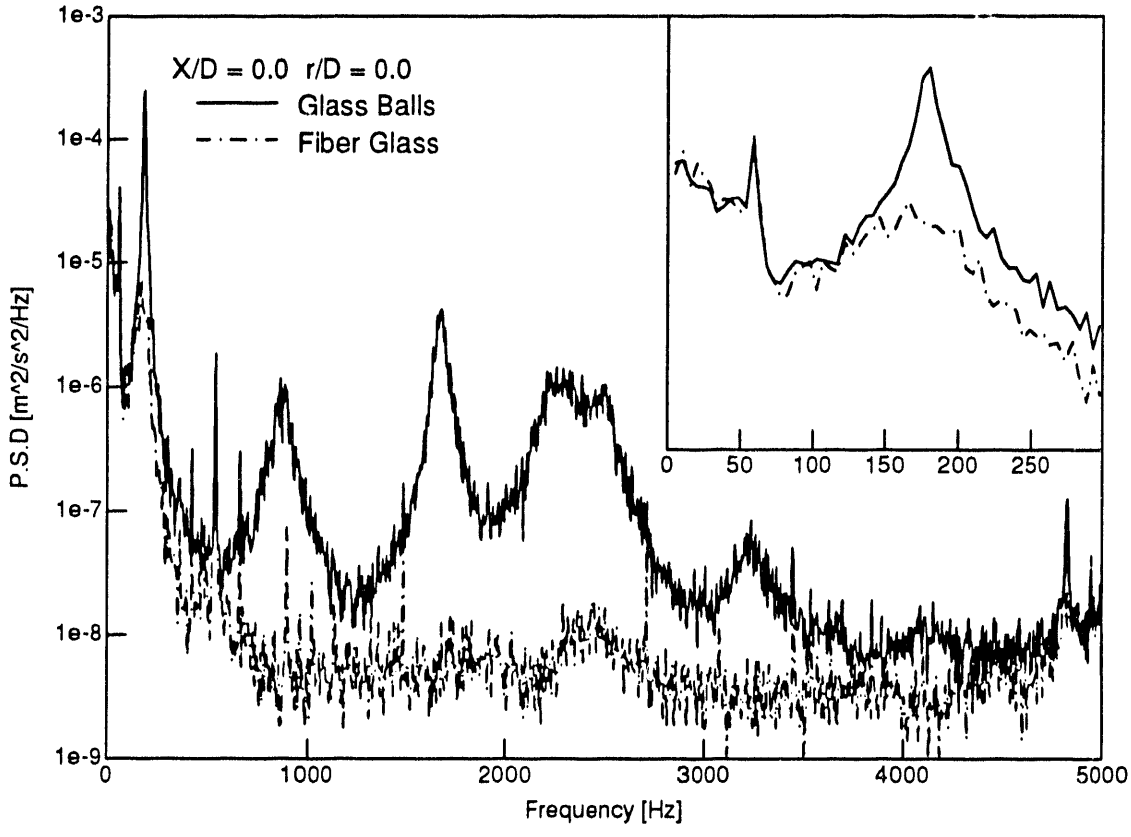

Figure 4 : Velocity spectra in isothermal conditions at the exit of the burner

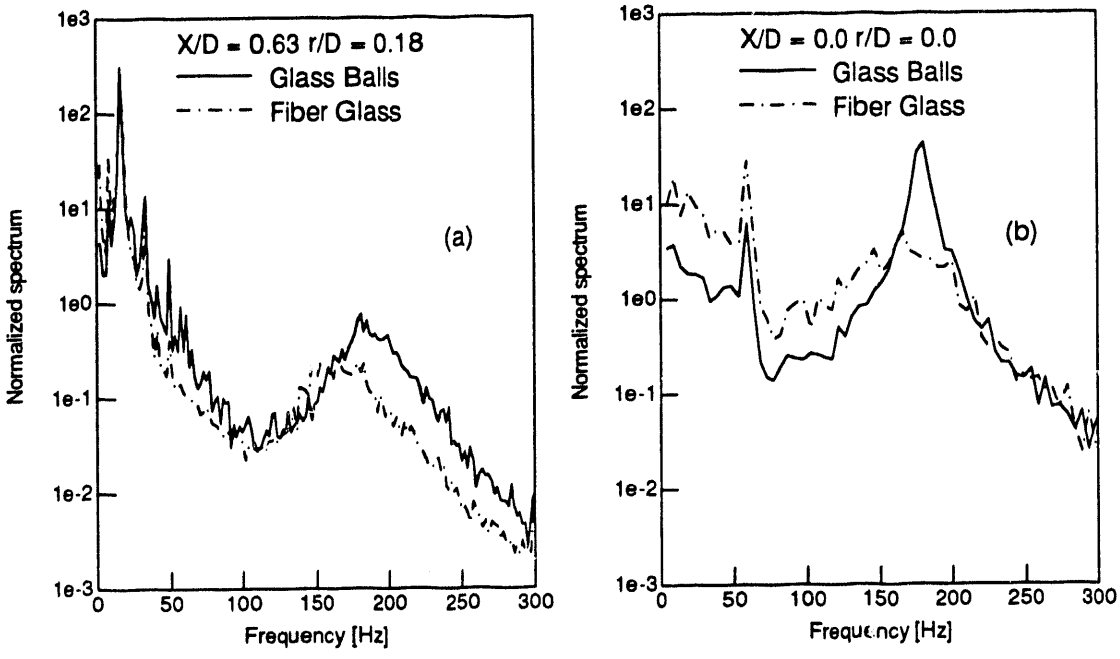

Figure 5 : Spectra in the flame front zone (a) beam deflection spectra, (b) acoustic velocity spectra

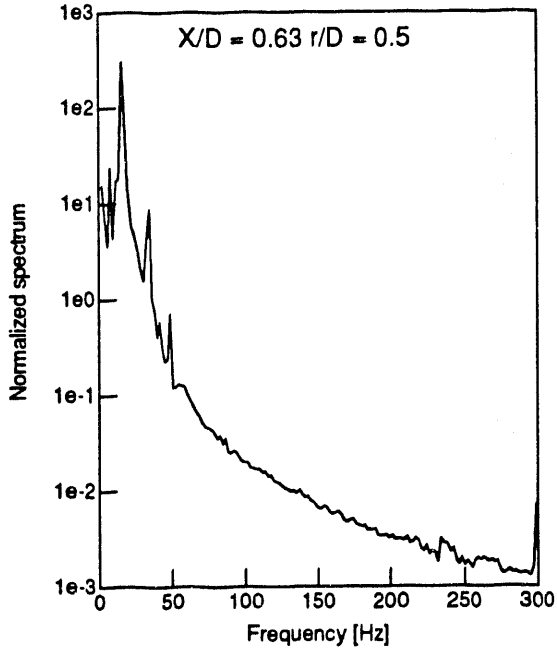

Figure 6 : Beam deflection spectrum in the interface product/air zone

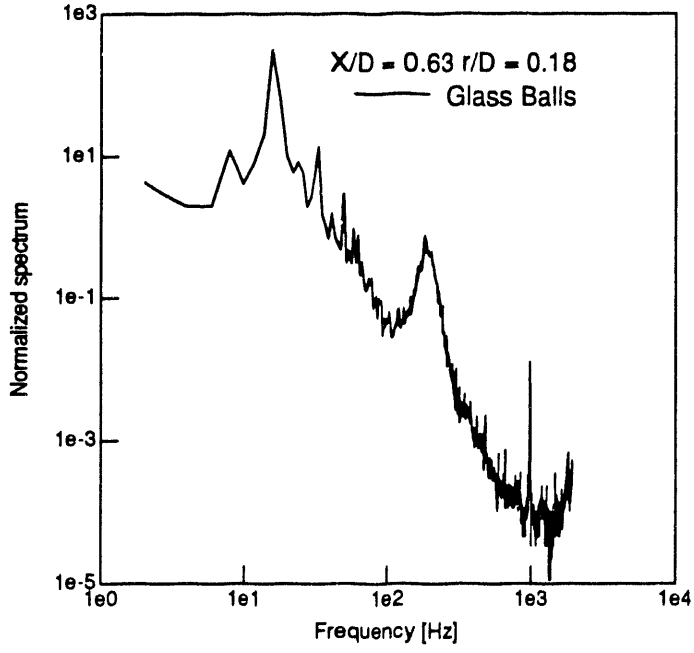

Fig 7 : Full beam deflection spectrum in the flame zone

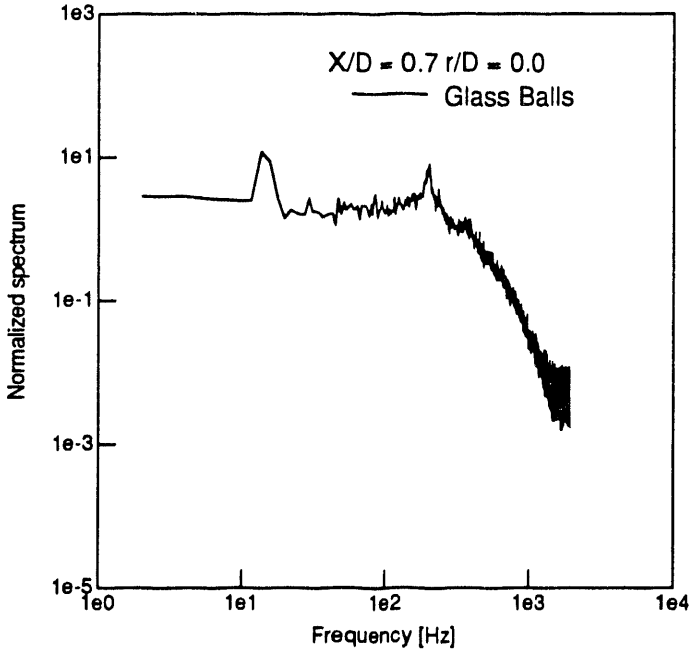

Fig 8 : Full beam deflection spectrum in the turbulent brush

DATE
FILMED
1 / 14 / 94
END